SOUTHERN HEMISPHERE STORM ZONES ON MARS: IMPLICATIONS OF MOLA TOPOGRAPHY.

J.L. Hollingsworth, *NASA Ames Research Center/SJSUF, MS 245-3, Moffett Field, CA 94035 (jeffh@humbabe.arc.nasa.gov)*, R.M. Haberle, *Space Science Division, NASA Ames Research Center, MS 245-3, Moffett Field, CA 94035*, J. Schaeffer, *Raytheon STX Corporation, Mountain View, CA 94035*.

Introduction: Using the NASA Ames Mars general circulation model [1, 2, 3] and recent Mars orbiter laser altimeter (MOLA) global topography [4], annual-cycle simulations have been performed corresponding to a low globally-averaged atmospheric dust loading ($\tau = 0.3$). Comparisons of key global circulation fields as simulated utilizing previous topography datasets [5] and those using the new Mars global topography have been carried out. Provided in Table 1 are values of globally and/or hemispheric averaged kinetic energy associated with the longitudinally averaged (i.e., zonal) circulation and longitudinal departures (i.e., eddy components) as a function of season for simulations using the different topography datasets. Here, the eddy terms include contributions arising from meteorological variability associated with thermal tides, stationary circulation components and recurrent weather systems (transient baroclinic and/or barotropic eddies). It can be noted that eddy activity in the northern hemisphere (NH) is substantially diminished using the new topographic data, and that at some seasons, the southern hemisphere (SH) activity is moderately increased.

L_s (°)	*Kinetic Energy*	*Smith-Zuber*	*MOLA*
90	zonal	3.15	2.82
180	zonal	2.10	2.28
270	zonal	4.55	4.40
360	zonal	2.16	2.17
90	NH eddy	0.30	0.24
90	SH eddy	0.45	0.46
180	NH eddy	0.53	0.49
180	SH eddy	0.53	0.57
270	NH eddy	1.14	0.77
270	SH eddy	0.46	0.43
360	NH eddy	0.74	0.55
360	SH eddy	0.27	0.30

Table 1: Global and hemispherically averaged kinetic energy ($\times 10^2$ m^2 s^2) associated with the atmospheric circulation as simulated by the NASA Ames Mars general circulation model.

Southern Late Autumn/Early Winter: Circulation statistics (e.g., variance/covariance of momentum and temperature) associated with midlatitude weather systems (transient baroclinic eddies) have been separated using band-pass time filtering [6] and analyzed for coherent spatial patterns during southern late autumn and early winter. A new finding from the NASA Ames Mars general circulation model (MGCM) simulation with MOLA topography is the occurrence of a weak (compared to the northern winter case [7, 8]) but organized 'storm zone'— a preferred longitudinal corridor for development and decay of the southern transient eddies. As shown in Figure 1, eddy activity is highly lo-

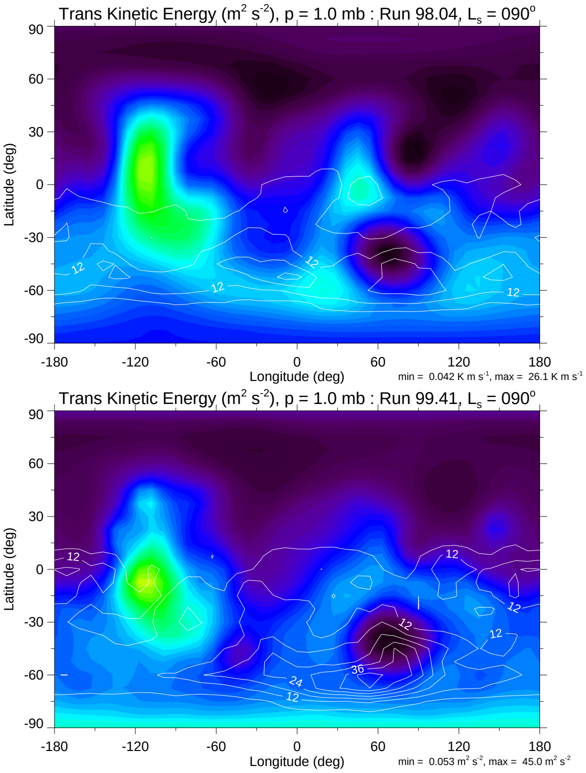

Figure 1: (a) A longitude-latitude cross section of the band-pass filtered transient eddy kinetic energy (m^s s^2) at p = 1.0 mbar as simulated by the NASA Ames Mars general circulation model for $L_s = 90°$ using the Smith and Zuber (1996) topography [4]. (b) as in (a) but with MOLA global topography [5]. In panels (a) and (b), the contour interval is 6 m^2 s^2 and the color shading denotes the topography datasets.

calized between the Argyre and Hellas basins. Such preferred geographic regions for eddy development and decay imply preferred regions for the transport of volatiles and dust.

Southern Early Spring: In contrast, during southern early spring as shown in Figure 2, transient eddy activity as measured by temporal variance and covariance fields of heat and momentum is significantly strong, and even exceeds that occurring in the northern hemisphere at this season. Past simulations using previous topography datasets have generally found very weak southern hemisphere transient eddy activity [8, 9]. Transient baroclinic eddies are active agents in the transport of heat, momentum and moisture in middle latitudes and thus variations in Mars' storm zones during the seasonal cycle have important implications for the planet's climate. The new simulations using MOLA topography suggest that the hemispheric asymmetry during the near-equinoctial season is not as pronounced as previously determined.

References: [1] Pollack J.B. et al. (1990) *J. Geophys. Res.* **95,** 1447–1474. [2] Haberle R.M. et al. (1993) *J. Geophys. Res.* **98,** 3093–3124. [3] Haberle R.M. et al. (1999) *J. Geophys. Res.* **104,** 8957–8974. [4] Smith D.E. et al. (1999) submitted to *Science*. [5] Smith D.E. and M.T. Zuber (1996) *Science* **271,** 184–188. [6] Trenberth K.E. (1991) *J. Atmos. Sci.*} **48,** *2159–2178. [7] Hollingsworth J.L. et al. (1996)* Nature **380,** *413–416. [8] Hollingsworth J.L. et al. (1997)* Adv. Space Res. **19,** *1237–1240. [9] Barnes J.R. et al. (1993)* J. Geophys. Res. **98,** *3125–3148.*

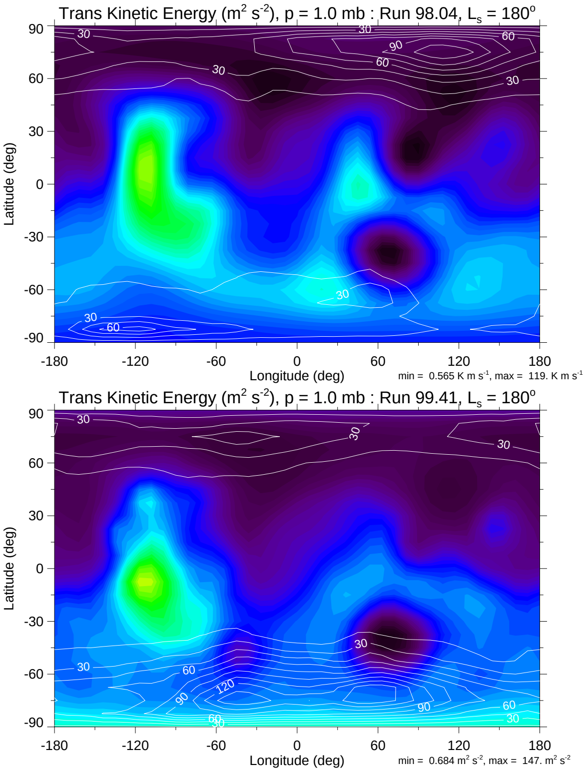

Figure 2: As in Figure 1 but for southern spring equinox conditions, $L_s = 180°$. In panels (a) and (b), the contour interval is 15 m^2 s^2 and the color shading denotes the topography datasets.